Proceedings of the 12th Asia Pacific Physics Conference
JPS Conf. Proc. **1**, 013108 (2014)

Cosmic Microwave Background B-mode Polarization Experiment POLARBEAR-2

Tomotake Matsumura[1], Peter Ade[2], Yoshiki Akiba[3], Christopher Aleman[4], Kam Arnold[4], Matt Atlas[4], Darcy Barron[4], Julian Borrill[6], Scott Chapman[5], Yuji Chinone[1], Ari Cukierman[7], Matt Dobbs[8], Tucker Elleflot[4], Josquin Errard[6], Giulio Fabbian[9], Guangyuan Feng[4], Adam Gilbert[8], William Grainger[10], Nils Halverson[11], Masaya Hasegawa[1], Kaori Hattori[1], Masashi Hazumi[1], William Holzapfel[7], Yasuto Hori[1], Yuki Inoue[3], Greg Jaehnig[11], Nobuhiko Katayama[12], Brian Keating[4], Zigmund Kermish[12], Reijo Keskitalo[6], Ted Kisner[6], Adrian Lee[7], Frederick Matsuda[4], Hideki Morii[1], Stephanie Moyerman[4], Michael Myers[7], Marty Navaroli[4], Haruki Nishino[12], Takahiro Okamura[1], Christian Reichart[7], Paul Richards[7], Colin Ross[5], Kaja Rotermund[5], Michael Sholl[7], Praween Siritanasak[4], Graeme Smecher[8], Nathan Stebor[4], Radek Stompor[9], Jun-ichi Suzuki[1], Aritoki Suzuki[7], Suguru Takada[14], Satoru Takakura[15], Takayuki Tomaru[1], Brandon Wilson[4], Hiroshi Yamaguchi[1], Oliver Zahn[7]

[1]*High Energy Accelerator Research Organization (KEK), Ibaraki, Japan*
[2]*Cardiff University, Cardiff, UK*
[3]*The Graduate University for Advanced Studies, Ibaraki, Japan*
[4]*University of California, San Diego, CA, USA*
[5]*Dalhousie University, Halifax, Canada*
[6]*Lawrence Berkeley National Laboratory, CA, USA*
[7]*University of California, Berkeley, Berkeley CA USA*
[8]*McGill University, Montreal, Canada*
[9]*Laboratoire Astroparticule et Cosmologie (APC), CNRS/IN2P3, Univ Paris Diderot, Paris, France*
[10]*Rutherford Appleton Laboratory, STFC*
[11]*Univeristy of Colorado, Boulder*
[12]*Kavli Institute for the Physics and Mathematics of the Universe (IPMU), Chiba, Japan*
[13]*Princeton University, NJ, USA*
[14]*National Institute for Fusion Science, Gifu, Japan*
[15]*University of Osaka, Osaka, Japan*

E-mail: tomotake.matsumura@kek.jp

(Received July 15, 2013)

POLARBEAR-2 (PB-2) is a ground-based experiment to measure the polarization of the cosmic microwave background (CMB) located at the Atacama desert (5200 m in altitude) in Chile. The science goals of the POLARBEAR-2 are i) to detect or set an upper limit of the inflationary gravitational wave B-mode with the sensitivity of $r = 0.01$ with 95 % C.L. and ii) to measure the weak gravitational lensing B-mode signal and extract the information, such as the sum of neutrino masses with the limit of 90 meV by PB-2 alone and 65 meV by combining PB-2 and Planck at 68 % CL. PB-2 observes at the 95 and 150 GHz bands simultaneously using the dichroic dual-polarization antenna-coupled transition edge sensor bolometers together with SQUIDs and the frequency domain multiplexing readout system. The total number of the detectors with the two bands are 7855 that are 6 times more than that of POLARBEAR-1, and the expected focal plane combined statistical sensitivity is 5.7 $\mu K\sqrt{s}$ with the beam size of 5.2 and 3.5 arcmin for the 95 and 150 GHz bands, respectively. The polarization signal is modulated by the sky rotation and the continuously rotating half-wave plate. PB-2 is scheduled to deploy in 2014. The PB-2 receiver will be mounted on the new telescope, which has the same design as the Huan Tran telescope (HTT). We present the overview of PB-2 and discuss the project status.

KEYWORDS: Cosmic microwave background radiation, Polarization, Inflation, Weak gravitational lensing

1. Introduction

The measurements of the cosmic microwave background (CMB) radiation have been playing a crucial role to establish the standard ΛCDM model in cosmology. The recent release of the cosmological results from the Planck temperature anisotropy measurements reveal the full sky picture of the last scattering surface up to the angular scale of $l \sim 2500$. While the standard cosmology looks well established, the inflationary paradigm and the nature of dark matter and dark energy are yet to be explored experimentally. The measurements of CMB polarization provide the means to probe the physics of the universe both before and after the last scattering surface.

The cosmological origin of the particular polarization pattern, called B-mode (as contrast to the E-mode originated from the primordial density perturbation), has potentially two sources, the primordial gravitational wave due to the inflation at the large angular scale, and the other, the conversion of CMB E-mode from the weak gravitational lensing via the large scale structure at small angular scale. As shown by a recent release of the cross-correlation result between the cosmic infrared background from a Herschel-SPIRE map and CMB lensing B-mode from SPT, a number of ground-based, balloon-borne, and satellite CMB polarization experiments are now chasing for these B-mode signals [1, 2].

POLARBEAR-2 (PB-2) is the ground-based CMB polarization experiment observing from the Atacama desert in Chile. PB-2 is sensitive to both the primordial gravitational wave B-mode and the weak lensing B-mode, and thus testing the inflationary paradigm and reconstructing mass potential at the late universe. In this paper we describe the instrumental overview and the current status.

2. Science goals and project overview

Figure 1 shows the CMB polarization power spectra with the projected sensitivities for PB-1, -2 and Planck [3–5]. The angular resolution of the telescope is 3.5 arcmin. at 150 GHz and thus PB-2 probes both large angular scale and small angular scale with the beam size and scan strategy. The PB-2 sensitivity with a fractional sky coverage of 20 % is designed to detect or set an upper limit on tensor-to-scalar ratio, $r = 0.01$, with 95% C.L. from the large angular scale. At smaller angular scale, PB-2 is sensitive to the gravitational lensing B-mode and the resultant sensitivity to the sum of neutrino masses via the mass potential reconstruction is 90 meV (67% C.L.) when only the PB-2 data are used and 65 meV (67% C.L.) when the PB-2 data are combined with the Planck data.

3. Instrument overview

Figure 2 shows Huan Tran telescope (HTT) that is located at the James Ax Observatory in the Atacama desert of Chile and the POLARBEAR-1 (PB-1) receiver is currently mounted. The new PB-2 receiver is designed to mount on a new telescope that has the same HTT design. The new receiver achieves higher optical throughput than that of PB-1 in two ways. One is to re-design the cryogenically cooled refractive optics and the receiver cryostat in order to increase the field-of-view from the existing 2.4 degrees in PB-1 to 4.8 degrees. The new receiver is designed to be compatible with the existing HTT design. The PB-2 detector employs the dichroic antenna-coupled Transition Edge Sensor (TES) bolometer [6]. This detector technology allows for a single pixel to observe the two frequencies, 95 GHz and 150 GHz simultaneously with two polarization states. Thus, each pixel corresponds to 4 bolometers. With these two approaches, the total number of the PB-2 bolometers is 6 times more than that of PB-1. The instrumental specifications of the PB-2 are summarized in Table I.

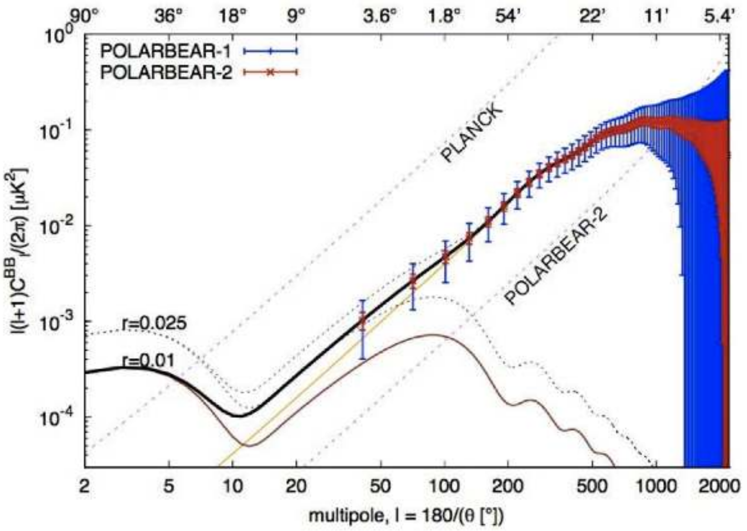

Fig. 1. The B-mode power spectra (ΛCDM model with two values of tensor to scalar ratio for primordial B-mode) are shown with the PB-1, PB-2 and Planck projected sensitivities.

Observing frequency	95 GHz	150 GHz
Number of pixels	1897 (3794 bolometers)	1897 (3794 bolometers)
NET array	500 $\mu K\sqrt{s}$	500 $\mu K\sqrt{s}$
NET array (temperature)	8.1 $\mu K\sqrt{s}$	8.1 $\mu K\sqrt{s}$
Beam size	5.2 arcmin.	3.5 arcmin.
Detector bath temperature	250 mK	
Field of view	4.8 degrees	
Observational time	3 years	

Table I. The PB-2 instrumental specifications.

3.1 Receiver

Figure 2 shows the 3D-CAD drawing of the receiver and a part of the actual receiver cryostat that is under testing. The receiver cryostat consists of two parts that share the vacuum, the receiver box (in analogy of its shape, a body part of the single-lens reflex camera) that stores the focal plane unit and readout electronics and the optics tube (lens in a single-lens reflex camera) that stores the cryogenically cooled refractive optics. The receiver has two pulse tube coolers to cool the receiver box and the optics tube simultaneously with a tilt angle of 21 degrees. When HTT points the sky at 45 degrees in elevation, the two PTCs are in level. For science observations, HTT is designed to point in elevation of 45 ± 40 degrees. Both the receiver box and the optics tube are built and in testing for vacuum and cryogenic performances.

3.2 Optics

HTT has an optical system of a two-mirror offset Gregorian with the 3 m × 2.5 m projected diameter primary and 1 m secondary mirrors with co-moving baffles. The secondary focus is re-imaged to achieve the telecentric focal plane by using the three cryogenically cooled lenses made of alumina in the receiver. Figure 3 shows the ray diagram of the optical system after the secondary mirror. We choose alumina with the 99.9 % purity as a lens material. Alumina is in polycrystal and no birefringence is expected. Use of alumna as a lens material has advantages in i) the higher index of refraction, $n \sim 3.1$, as compared to conventional millimeter-wave lens material such as UHMWPE ($n \sim 1.5$), ii) availability in size (up to 800 mm in diameter and 50 mm in thickness), and iii) higher

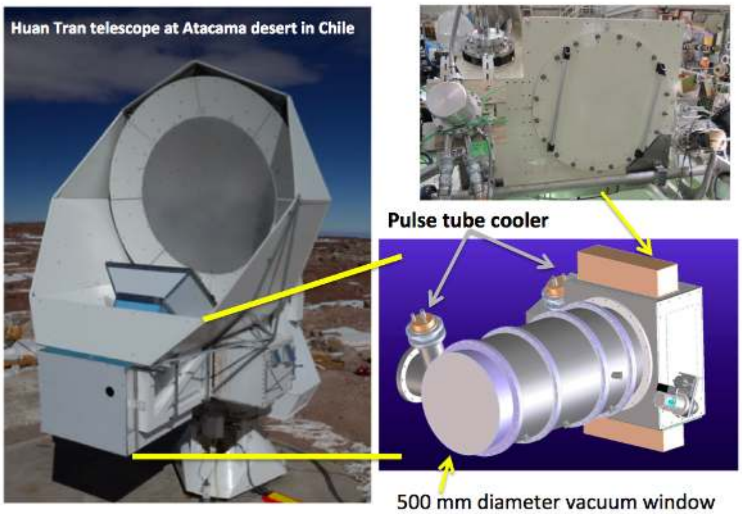

Fig. 2. Left: The Huan Tran telescope at the Atacama desert in Chile with the PB-1 receiver. Bottom right: The 3D-CAD drawing of the PB-2 receiver. Top right: A part of the constructed PB-2 receiver is shown in the picture.

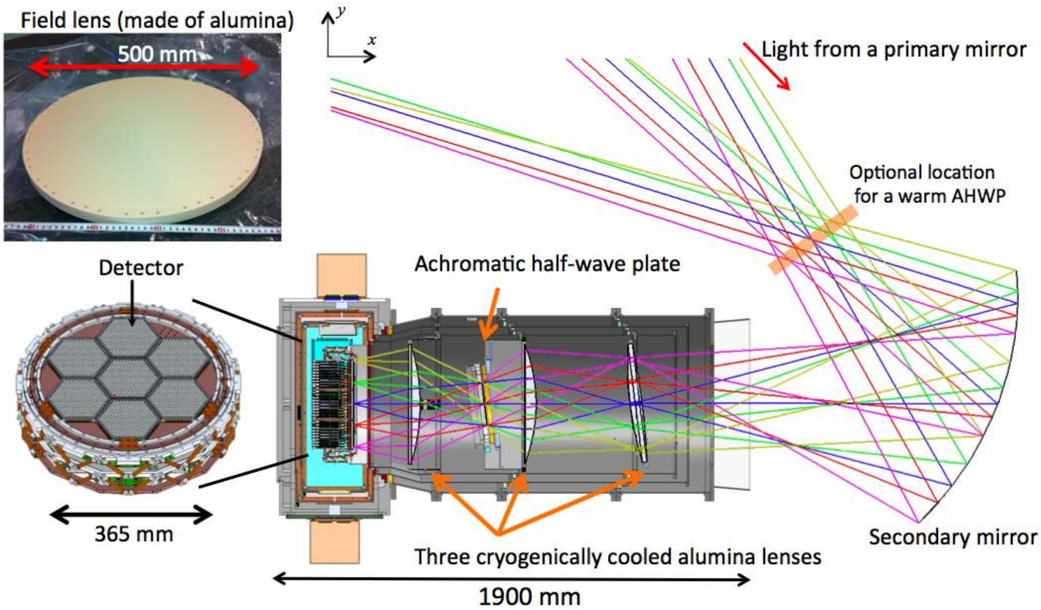

Fig. 3. Right: The ray diagram with the secondary mirror and receiver cryostat. Top left: The alumina field lens. Bottom left: The 3D-CAD of the focal plane unit that is under fabrication.

thermal conductivity. The measured loss-tangent of a 99.9 % purity alumina is $\tan\delta \sim 2\times10^{-4}$ at the temperature of 77 K. The detailed descriptions of alumina properties are in the Inoue's thesis [8].

The large optical throughput with a fixed $F/\#$ to the receiver forces to have a window diameter of 500 mm. While we prepare a window made of zotefoam, we also explore the option of actively cooled window to reduce the thermal radiation from the window itself. Due to the large entrance window, it is essential to have a proper infrared (IR) blocking filter. We develop a new absorptive filter using a base material of alumina. This alumina filter is placed at the 50 K stage to absorb the incident IR radiation and conduct the heat away with a high thermal conductance of alumina. The detailed

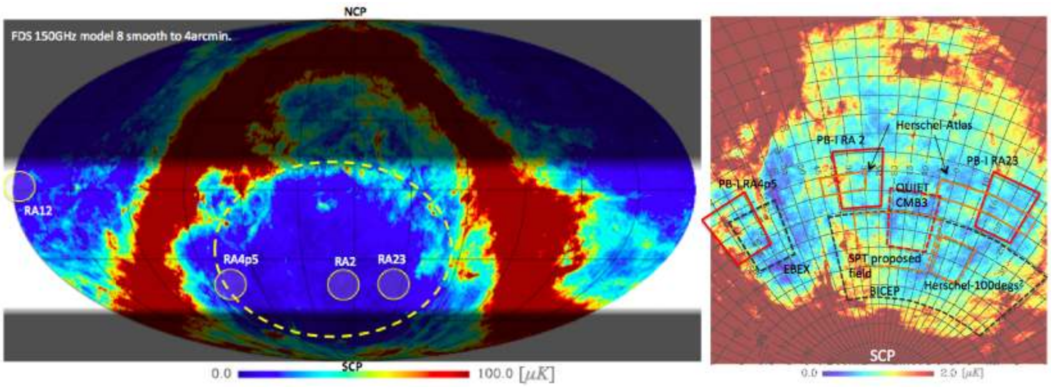

Fig. 4. Left: The dust foreground based on FDS model 8 at 150 GHz is shown. The observable range from the Atacama desert in Chile is shown as a non-darker area. The circles indicated the regions PB-1 is observing. The dashed circle is the low dust contract region where PB-2 will observe. Right: The zoomed southern hole (the dashed circle in left panel) region with the observed patches by various experiments.

description of alumina IR filter is in Inoue et al. [9]. In the entire optical and cryogenic chains, PB-2 uses three types of IR filters, alumina filter at the 50 K stage, metal mesh filter and alumina lenses at the 4 K stage [10]. Alumina lenses also serve as an IR filter.

The higher index of refraction of alumina and silicon for optical elements requires a proper anti-reflection (AR) coating. The dielectric constant of epoxy based glue matches to the required AR coating index. Therefore, PB-2 uses two layer epoxy based glue for the AR coating and the expected transmission at 95 (150) GHz band is 2 % (4 %) for the alumina filter and 10 (15 %) per lens [6] .

The polarization is modulated by the sky rotation and the cryogenically cooled continuously rotating half-wave plate (HWP). An achromatic HWP (AHWP) is installed at aperture in the receiver and kept at 4 K to minimize the thermal emission. We have an option of placing a room temperature AHWP at the prime focus as shown in Figure 3. The AHWP using three sapphire layers covers the modulation efficiency of > 0.99 at the observing bands and test using a prototype test is underway. The detailed PB-2 optics and polarimeter system are described in Matsumura et al. [11].

3.3 Detector and readout system

PB-2 employs the 7588 dichroic dual-polarization antenna-coupled TES bolometers. Figure 3 shows the focal plane unit that consists of seven wafers and each has 271 pixels, i.e. 1084 bolometers. The detailed descriptions of the PB-2 TES bolometers and its implementation are in Suzuki et al. [6, 7].

The signal is read by the Superconducting Quantum Interference Device (SQUID) and digital frequency multiplex readout system with the multiplexing factor of 32. As the total number of the detector increases it is important to have higher multiplexing factor. In order to pack the frequency comb within the available bandwidth it is essential to minimize the stray inductance along the signal line. PB-2 employs the digital active nulling to minimize the stray inductance. Hattori et al. describes the adaptation of the DfMUX system to the PB-2 TES detector system [12].

We develop multiple detector test cryostat systems that each system has a 300 mK temperature stage and has a capability to test a single detector wafer. The test cryostat is much smaller than that for the science observations. Therefore, we can test multiple detector wafer and readout systems in parallel with a shorter turnaround time of a cryostat run.

4. Observation and systematic effects

Figure 4 shows the observable part of the sky from the Atacama desert in Chile within the elevation range of $30 < el < 80$ degrees. The regions PB-1 currently observe are optimized for i) minimal dust RMS based on the FDS model 8, ii) overlaps with other observations for cross-correlation anal-

Systematic error	Requirement	Further mitigation
Differential gain	0.1 %	Continuous HWP
Differential pointing	0.8 arcsec	Continuous HWP
Differential beam ellipticity	3 %	Continuous HWP
Differential beam size	2 %	Continuous HWP
Polarization angle	0.25 degs	External polarized sources

Table II. The systematic effect requirements. The values are for the case with a stepped HWP. The continuous rotating HWP provides the further mitigation of the systematic effects.

ysis, and iii) longest observational time [13]. PB-1 observes the patches with the constant elevation scan and PB-2 follows the same strategy with the fractional sky coverage of 20 %.

Table II shows the benchmark requirement of the systematic errors estimated by the semi-analytic formalism [14]. The systematic error requirement is determined by requiring that each systematic contribution is less than the primordial B-mode signal of $r = 0.001$ at $l = 90$. The requirement of the differential beam size and ellipticity are determined by setting the same condition not to the primordial B-mode signal but the lensing B-mode at $l = 1000$. The values are already taken into account the mitigation due to the available sky rotation at Chile and the stepped HWP rotation. The further mitigation is expected with the continuously rotating HWP.

5. Conclusions

The PB-2 upgrade is designed to measure the CMB polarization signal from inflation for $r = 0.01$ (95 %) and the weak gravitational lensing B-mode signal. The sensitivity to the latter signal results the sum of neutrino masses, $\sigma(\sum m_\nu) < 90$ meV with PB-2 alone and 65 meV with PB-2 and Planck together. The PB-2 re-imaging optics and receiver are re-designed from that of PB-1 in order to increase the optical throughput, and the corresponding research and development in optics, cryogenics, detector technologies are in progress. PB-2 is scheduled to deploy in 2014 to the new Huan Tran telescope at the Atacama desert in Chile.

Acknowledgements

Support from the MEXT Kakenhi grant 21111002, 24740182, 24111715, NSF grant AST-0618398, NASA grant NNG06GJ08G, Simons Foundation, Natural Sciences and Engineering Research Council, Canadian Institute for Advanced Research and the CONICYT. Detectors were fabricated at Berkeley nanofabrication laboratory.

References

[1] T. Matsumura, Proceedings of Rencontres du Blois, 2012.
[2] Hunson et al., Phys. Rev. Lett. 111, 141301.
[3] Z. Kermish et al., Proceedings of SPIE Volume 8452, 2012.
[4] T. Tomaru et al., Proceedings of SPIE Volume 84521H, 2012.
[5] Planck collaboration, Planck 2013 results. I. Overview of products and scientific results.
[6] Aritoki Suzuki et al., Proceedings of SPIE Volume 8452, 2012.
[7] Aritoki Suzuki et al., Proceedings of LTD15, 2013.
[8] Y. Inoue,The thermal design of the POLARBEAR-2 experiment. Master. thesis, The Graduate University for Advanced Studies, 2012. (http://cmb.kek.jp/sub9.html)
[9] Y. Inoue et al., Cryogenic infrared filter using alumia for use at millimeter wavelength, Submitted to Applied Optics.
[10] P. Ade, A Review of Metal Mesh Filters, Proc. of SPIE Vol. 6275 62750U-1.
[11] T. Matsumura et al., Proceedings of SPIE Volume 84523E, 2012.
[12] K. Hattori et al., Proceedings of VCI 2013.
[13] Finkbeiner, D. P., Davis, lVI., & Schlegel, D. J. 1999, Astrophys. J. ,524,867, astro-ph/9905128.
[14] Shimon et al., Phys.Rev.D77:083003,2008, astro-ph/0709.1513.